Chaos and Regularity in the Doubly Magic Nucleus ^{208}Pb

B. Dietz,[1,†] A. Heusler,[2,‡] K. H. Maier,[3,*] A. Richter,[4,§] and B. A. Brown[5,¶]

[1]School of Physical Science and Technology, and Key Laboratory for Magnetism and Magnetic Materials of MOE, Lanzhou University, Lanzhou, Gansu 730000, China

[2]Gustav-Kirchhoff-Strasse 7/1, D-69120 Heidelberg, Germany

[3]Institute of Nuclear Physics, Polish Academy of Sciences, 31-342 Kraków, Poland

[4]Institut für Kernphysik, Technische Universität Darmstadt, D-64289 Darmstadt, Germany

[5]Department of Physics and Astronomy and National Superconducting Cyclotron Laboratory, Michigan State University, East Lansing, Michigan 48824-1321, USA

(Received 20 July 2016; revised manuscript received 8 November 2016; published 3 January 2017)

High-resolution experiments have recently lead to a complete identification (energy, spin, and parity) of 151 nuclear levels up to an excitation energy of $E_x = 6.20$ MeV in ^{208}Pb [Heusler *et al.*, Phys. Rev. C **93**, 054321 (2016)]. We present a thorough study of the fluctuation properties in the energy spectra of the unprecedented set of nuclear bound states. In a first approach, we group states with the same spin and parity into 14 subspectra, analyze standard statistical measures for short- and long-range correlations, i.e., the nearest-neighbor spacing distribution, the number variance Σ^2, the Dyson-Mehta Δ_3 statistics, and the novel distribution of the ratios of consecutive spacings of adjacent energy levels in each energy sequence, and then compute their ensemble average. Their comparison with a random matrix ensemble which interpolates between Poisson statistics expected for regular systems and the Gaussian orthogonal ensemble (GOE) predicted for chaotic systems shows that the data are well described by the GOE. In a second approach, following an idea of Rosenzweig and Porter [Phys. Rev. **120**, 1698 (1960)], we consider the complete spectrum composed of the independent subspectra. We analyze their fluctuation properties using the method of Bayesian inference involving a quantitative measure, called the chaoticity parameter f, which also interpolates between Poisson ($f = 0$) and GOE statistics ($f = 1$). It turns out to be $f \approx 0.9$. This is so far the closest agreement with a GOE observed in the spectra of bound states in a nucleus. The same analysis is also performed with spectra computed on the basis of shell model calculations with different interactions (surface-delta interaction, Kuo-Brown, Michigan-three-Yukawa). While the simple surface-delta interaction exhibits features typical for nuclear many-body systems with regular dynamics, the other, more realistic interactions yield chaoticity parameters f close to the experimental values.

DOI: 10.1103/PhysRevLett.118.012501

Introduction.—The stable doubly magic nucleus ^{208}Pb is one of the most studied nuclei both experimentally and theoretically. Many of its spectral properties are basically understood in terms of the nuclear shell model. In recent years, however, a number of high-resolution experiments using various types of nuclear reactions have been performed [1–4]. The foremost result is that now the complete level scheme in ^{208}Pb is established up to an excitation energy of $E_x = 6.20$ MeV comprising 151 bound states, of which the energy, spin, and parity have been unambiguously determined [1]. More states with spin and parity $J^\pi = 1^-, 2^-, 3^-$ are known up to $E_x \approx 7.5$ MeV [2–4]. In Fig. 1, the experimental levels are shown separately for states of negative (a) and positive (b) parity for a range of excitation energies $3.8 < E_x < 6.40$ MeV. Levels corresponding to states with natural and unnatural parity are shown as solid diamonds and open squares, respectively.

The level scheme of ^{208}Pb has also been the subject of many shell model calculations of the one-particle-one-hole and two-particle-two-hole type [5–17]. Mostly, the coupling of proton particles in the orbitals $1h_{9/2}$, $2f_{7/2}$, $2f_{5/2}$, $3p_{3/2}$, $3p_{1/2}$, and $1i_{13/2}$ to proton holes in the orbitals $1g_{7/2}$, $2d_{5/2}$, $2d_{3/2}$, $3s_{1/2}$, and $1h_{11/2}$ and the coupling of neutron particles in the orbitals $1i_{11/2}$, $2g_{9/2}$, $2g_{7/2}$, $3d_{5/2}$, $3d_{3/2}$, $4s_{1/2}$, and $1j_{15/2}$ to neutron holes in the orbitals $1h_{9/2}$, $2f_{7/2}$, $2f_{5/2}$, $3p_{3/2}$, $3p_{1/2}$, and $1i_{13/2}$ were taken into account; see, e.g., Fig. 1 of Ref. [18]—however, note the different labelings used for the main quantum number. For detailed level schemes of the relevant proton and neutron orbits in the four neighboring nuclei of ^{208}Pb, see, e.g., Fig. 1 in Ref. [1] or Fig. 3–3 in Ref. [19]. The calculations of Kuo and Brown (KB) use four additional orbitals [5–8]. In total, there are 27 different combinations of spin and parity for one-particle-one-hole states in ^{208}Pb. The surface-delta interaction (SDI), which acts only at the nuclear surface, has been introduced as a simple extension of the schematic shell model without a residual interaction. The associated interaction strength depends on the atomic mass number as the ratio of the surface to the volume term and on geometrical recoupling coefficients [15–17]. The KB interaction is based on the free nucleon-nucleon potential of Hamada and Johnston [5–8]

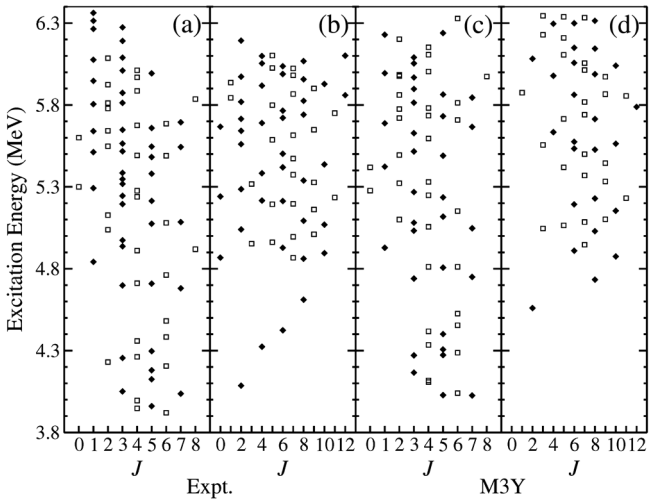

FIG. 1. Experimental levels for states in ^{208}Pb at $3.8 < E_x < 6.4$ MeV with negative parity (a) and positive parity (b). They are compared to the levels calculated for the M3Y residual interaction with negative parity (c) and positive parity (d). Solid diamonds and open squares show the levels with natural and unnatural parity, respectively.

and the more recent two-body Michigan-three-Yukawa (M3Y) interaction on a one-boson exchange potential with short-range components determined with the help of the Reid nucleon-nucleon potential [12–14]. Figure 1 shows the excitation energies calculated with the shell model which employs the effective nucleon-nucleon interaction M3Y for negative (c) and positive (d) parity.

The main objective of the present Letter is *not* a level by level comparison but rather a comparison of the spectral properties of the whole set of detected bound states in ^{208}Pb up to an excitation energy of $E_x = 6.20$ MeV, which is still about one MeV below the neutron threshold [$S(n) = 7.368$ MeV], and of the three theoretical models with random matrix theory (RMT) results. For a generic quantum system with classically regular dynamics, the spectral properties are predicted to coincide with those of Poissonian random numbers [20]. According to the Bohigas-Giannoni-Schmit conjecture [21], the spectral properties of time-reversal-invariant chaotic systems are well described by those of the eigenvalues of real-symmetric matrices with Gaussian distributed random entries from the Gaussian orthogonal ensemble (GOE) [22–26]. These features are also observed in nuclear many-particle systems with no obvious classical analogue. Their spectral properties are described by Poissonian statistics, if the motion of the particles is collective, whereas for sufficiently complex motion they exhibit GOE statistics [27–30]. There are various methods to obtain information on the chaoticity vs regularity in a nuclear many-body system from its spectrum; see, e.g., the review articles [30,31]. We analyzed the fluctuation properties of the energy levels using two models, where one is based on a RMT ensemble [32–34] and the other one on the method of Bayesian inference [35–37]. Both provide quantitative measures for the chaoticity in terms of a parameter which interpolates between the Poisson statistics and GOE statistics.

Spectral data.—We note that, besides for ^{208}Pb, there are to our knowledge only two other nuclei for which complete level schemes exist, namely, ^{26}Al and ^{30}P [38–40]. That of ^{116}Sn has been termed "nearly complete" by the authors of Refs. [41,42]. Furthermore, the analysis of the spectral properties of experimentally determined bound states of nuclei did not yield the results expected in nuclear many-body systems exhibiting a chaotic dynamics. For light nuclei this was attributed to the insufficient number of identified bound states, and for nuclei like ^{26}Al and ^{30}P to the partial isospin symmetry breaking [38,39]. The present analysis of the experimental data is based on the 151 bound states with unambiguously assigned parity and spin [1], so the results are statistically significant.

We applied two different approaches to analyze the spectral fluctuation properties of the experimental data [1–4] and calculations [5–12,15–17]. In the first approach, we determined the ensemble averages of the statistical measures for the spectral properties of each level sequence [43] characterized by spin and parity. In the second approach, we followed an idea of Rosenzweig and Porter [44] and considered the complete spectrum composed of the independent subspectra and analyzed their fluctuation properties using the method of Bayesian inference. Note that the spectral properties are Poissonian, when we use the complete experimental spectrum irrespective of parity and spin; see Fig. 6 of Ref. [45]. In both approaches, we considered only subspectra that contained at least five levels. Furthermore, we first unfolded the energy levels E_i in each sequence individually by replacing them by the smooth part $\overline{N}(E_i)$ of the integrated level density, yielding a mean spacing of unity $\langle s \rangle = 1$. The latter was determined from a fit of a third-order polynomial to the integrated level density. In order to assure ourselves that the spectral properties do not depend on the unfolding procedure, we, in addition, unfolded the energy levels using an empirical formula [46,47], $\overline{N}(E) = \exp[(E - E_0)/T] + N_0$ with T, E_0, and N_0 the fit parameters. It was applied to low-lying nuclear levels in Ref. [48]. We came to the result that both procedures yield very similar results for the fluctuations of the energy levels.

Ensembles of subspectra.—In order to get information on the chaoticity of the nuclear many-body system we calculated for each sequence of unfolded levels (i) the nearest-neighbor spacing distribution (NNSD) $P(s)$, (ii) the number variance Σ^2, (iii) the Dyson-Mehta Δ_3 statistics [25,26] which gives the least-square deviation of the integrated level density from the best-fit straight line, and (iv) the distribution of the ratios of the consecutive spacings of adjacent energy levels [49,50], which has the advantage that the energy levels need not be unfolded. The corresponding analytical expressions for Poisson and GOE statistics are given in Refs. [25,26,49].

TABLE I. The number of sets m and spacings N for the composite experimental (Exp.) spectra (All), positive (+) and negative (−), natural (Nat.) and unnatural (Unnat.) parity, and for those calculated with three different models. The numbers N are larger for the models than for the experimental data, because we had levels with energies larger than 6.2 MeV at our disposal. The chaoticity parameter and its variance $f = \bar{f} \pm \sigma$ were obtained with the method of Bayesian inference [Eqs. (3) and (5)]. The chaoticity parameter λ was obtained with the RMT model Eq. (1), and σ_λ gives the mean-square deviation of the respective NNSD from the corresponding analytical expression Eq. (2).

Model	Parity	m	N	$\bar{f}$	σ	λ	σ_λ
Exp.	All	14	128	0.95	0.015	1.50	0.060
SDI	All	13	262	0.18	0.069	0.08	0.001
M3Y	All	13	282	0.73	0.066	0.64	0.053
KB	All	14	257	0.62	0.070	0.60	0.074
Exp.	+	7	45	0.94	0.033	1.70	0.140
SDI	+	6	82	0.05	0.042	0.01	0.010
M3Y	+	6	84	0.84	0.079	1.13	0.081
KB	+	4	62	0.88	0.059	1.50	0.118
Exp.	−	7	83	0.87	0.091	0.70	0.093
SDI	−	7	180	0.10	0.062	0.05	0.025
M3Y	−	7	198	0.66	0.085	0.64	0.057
KB	−	10	295	0.62	0.070	0.50	0.079
Exp.	Nat.	5	79	0.92	0.051	1.20	0.096
SDI	Nat.	7	136	0.16	0.087	0.05	0.001
M3Y	Nat.	7	147	0.80	0.073	0.75	0.094
KB	Nat.	7	169	0.74	0.091	1.10	0.085
Exp.	Unnat.	6	49	0.89	0.084	2.00	0.120
SDI	Unnat.	6	126	0.09	0.063	0.10	0.001
M3Y	Unnat.	6	135	0.65	0.096	0.58	0.089
KB	Unnat.	6	188	0.62	0.088	0.50	0.079

We analyzed the statistical measures for the experimental energy levels and for the levels obtained from nuclear model calculations using the SDI, M3Y, and KB interactions for each of the m subspectra separately and subsequently computed their ensemble averages, where the values of m are given in Table I. Then we compared them to those of random matrices from an ensemble interpolating between Poisson and the GOE [32,34]:

$$H(\lambda) = (H_0 + \lambda H_1)/\sqrt{1+\lambda^2}, \quad (1)$$

where H_0 is a diagonal matrix of random Poissonian numbers and H_1 is a matrix from the GOE. Here, the range of values of the entries of H_0 coincided with that of the eigenvalues of H_1. Furthermore, the variances of the matrix elements of H_0 and H_1 were chosen such that the mean spacings of their eigenvalues equaled unity, respectively. For $\lambda = 0$ the statistics is Poissonian, whereas for $\lambda \gtrsim 1$ the statistical properties are close to those of random matrices from the GOE. In Ref. [32], a Wigner-like approximation was derived for the NNSD using 2×2 random matrices. It is given in terms of the Bessel function $I_0(x)$ and the Kummer function $U(a,b,x)$ as

$$P_{P\to\mathrm{GOE}}(s,\lambda) = su(\lambda)^2/\lambda \exp\left[-u(\lambda)^2 s^2/4\lambda^2\right] \times \int_0^\infty d\xi e^{-\xi^2-2\xi\lambda} I_0[\xi s u(\lambda)/\lambda], \quad (2)$$

with $u(\lambda) = \sqrt{\pi}U(-1/2, 0, \lambda^2)$. In order to determine the parameters λ for the experimental and calculated spectra, we fit this expression to their NNSDs and also compared their Σ^2 statistics with that obtained for the RMT model Eq. (1) around the respective λ values. The inclusion of long-range correlations turned out to be crucial for the determination of the best-fit parameters. The λ values and the mean-square deviation of the respective NNSD from the analytical one, σ_λ, are given in the last two columns in the rows termed "All" in Table I. We repeated the analysis taking into account only levels with positive, negative, natural ($J^\pi = 1^-, 2^+, \ldots$), and unnatural ($J^\pi = 0^-, 1^+, 2^-, \ldots$) parity, respectively. This analysis clearly revealed that the spectral properties of the experimental levels are very close to the GOE. The NNSDs for the M3Y and the KB interaction models are also close to the GOE; however, their Σ^2 statistics hint at a slightly larger contribution from regular behavior than for the experimental ones. Interestingly, for all these cases the spectra of levels with positive or natural parity are closer to the GOE than those with negative and unnatural parity, respectively. The SDI model, on the contrary, clearly exhibits Poissonian features. We illustrate the findings in Figs. 2–4, where we compare the NNSD, the Δ_3 statistics, and the ratio distributions of the experimental and calculated levels (histograms and circles) with those of Poissonian random numbers (dash-dotted lines) and of random matrices from the GOE (dashed lines). Furthermore, Figs. 3 and 4 show the results (red histogram and dots) obtained from the RMT model Eq. (1) using the λ values given in Table I; see also Figs. 1–3 of Ref. [45]. A second measure for the chaoticity vs regularity is analyzed in the next section.

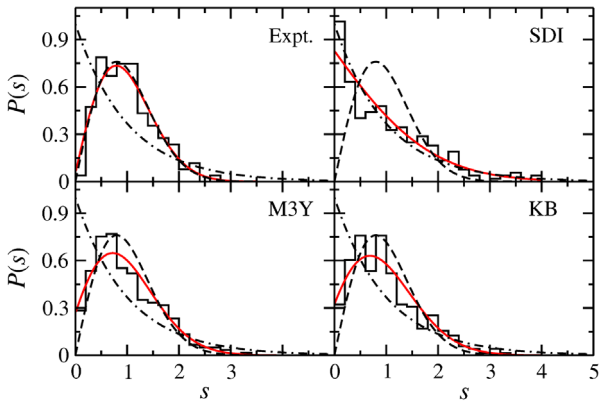

FIG. 2. Nearest-neighbor spacing distribution of all experimental and calculated energy levels, respectively (histograms). They are compared to the Poisson (dash-dotted line) and the GOE (dashed line) distribution. The solid curves in red were determined with the method of Bayesian inference [Eqs. (3) and (5)].

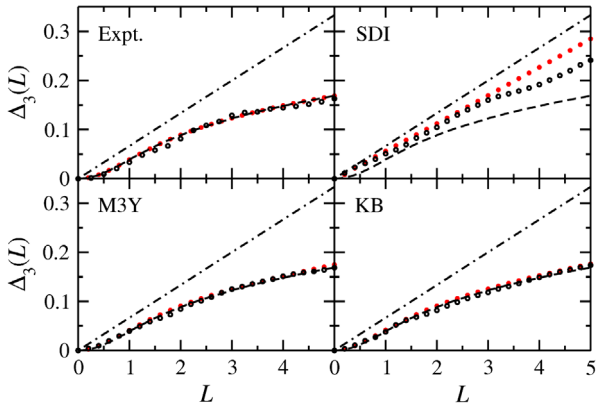

FIG. 3. The Dyson-Mehta statistics of all experimental and calculated energy levels, respectively (black circles), in comparison to the Poisson (dash-dotted line) and GOE (dashed line) results, and the RMT model Eq. (1) for the corresponding best-fit parameter λ (red dots).

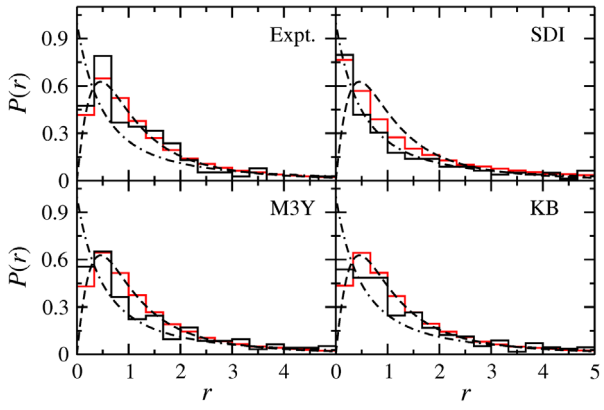

FIG. 4. Ratio distributions of all experimental and calculated energy levels, respectively (black histogram), in comparison to the Poisson (dash-dotted line) and GOE (dashed line) results, and the RMT model Eq. (1) for the corresponding best-fit parameter λ (red histograms).

Superimposed subspectra.—For the analysis of the composite spectra, we proceeded as described in Refs. [35–37]. Accordingly, we first computed the spacings between adjacent unfolded energy levels in each subspectrum separately and then merged them irrespective of spin and parity into one sequence of spacings $s_i, i = 1, \ldots, N$ with N given in Table I. An approximate expression was derived for the NNSD $p(s, f_1, \ldots, f_m)$ of a spectrum composed of m subspectra with fractional level numbers $0 < f_j \leq 1$, $j = 1, \ldots, m$, in Ref. [44]. In Ref. [35], an approximation was derived which depends only on one parameter $f = \sum_{j=1}^{m} f_j^2$ and is given by

$$p(s,f) = \left(1 - f + \frac{\pi}{2} Q(f) s\right) \exp\left(-(1-f)s - \frac{\pi}{4} Q(f) s^2\right) \tag{3}$$

with $Q(f) = 0.7f + 0.3f^2$. Note that for $f = 0$, which corresponds to a spectrum composed of a large number of subspectra consisting of a few number of levels, this distribution approaches the Poisson distribution, whereas for $f \to 1$ it converges to the NNSD of the GOE. Therefore, f is referred to as the chaoticity parameter.

In order to determine the values of f for the experimental and calculated composite spectra, we used the method of Bayesian inference [51]. Assuming that the spacings $s_j, j = 1, \ldots, N$, are statistically independent, their joint probability distribution can be written as the product

$$p(\boldsymbol{s}|f) = \prod_{j=1}^{N} p(s_j, f), \tag{4}$$

where we used the notation $\boldsymbol{s} = (s_1, s_2, \ldots, s_N)$ and $p(s_i, f)$ is given by Eq. (3). The assumption, actually, restricts the applicability of the approach to short-range correlation functions. According to Bayes' theorem, the posterior distribution of the parameter f for a given sequence of spacings $\boldsymbol{s}$ is given as

$$P(\boldsymbol{s}|f) = \frac{p(\boldsymbol{s}|f)\mu(f)}{\mathcal{N}(\boldsymbol{s})}, \tag{5}$$

where $\mu(f)$ is the prior distribution of f and $\mathcal{N}(\boldsymbol{s})$ is the normalization constant. Using Jeffrey's rule [51–53], an approximate expression was derived for $\mu(f)$ in Ref. [36], $\mu(f) = 1.975 - 10.07f + 48.96f^2 - 135.6f^3 + 205.6f^4 - 158.6f^5 + 48.63f^6$. To determine the chaoticity parameter f, we computed the joint probability distribution of the spacings $p(\boldsymbol{s}|f)$ for $0 \leq f \leq 1$ using Eq. (3). The best-fit value of f was then obtained as the mean value $\overline{f} = \int_0^1 f P(\boldsymbol{s}|f) df$, which gives the fraction of subspectra that exhibit GOE behavior with variance σ, $f = \overline{f} \pm \sigma$, where $\sigma^2 = \int_0^1 (f - \overline{f})^2 P(\boldsymbol{s}|f) df$ provides a measure for the uniformity of chaoticity in the ensemble of subspectra. This yielded the values of $\overline{f}$ and σ listed in Table I for the experimental and calculated spectra. They are in line with those obtained with the RMT model Eq. (1). The corresponding NNSDs are shown as red curves in Fig. 2 and in Fig. 4 of Ref. [45].

Results, discussion, and conclusion.—Table I summarizes the results of the analysis of the recently completed level scheme of ^{208}Pb at $E_x \lesssim 6.20$ MeV together with complementary results from calculations. For the experimental and the calculated spectra of the nuclear models with M3Y and KB interactions, the chaoticity parameters f and λ indicate that the spectral properties are described by the GOE, even though there seems to be some small admixture from regular dynamics in the latter two cases. The chaoticity parameters for the SDI, on the contrary, suggest a behavior which is close to Poisson statistics. In a second step, the same analysis has been applied to the spectra of energy levels with positive, negative, natural, and

unnatural parity, respectively. Albeit the sample sizes of m and N are smaller, the chaoticity parameters for the experimental spectra and for those calculated with the M3Y and KB interactions again are close to the values of GOE statistics. Note that the parameters are closer to that for a pure GOE for levels with positive and natural parity than for those with negative and unnatural parity. In contrast, all chaoticity parameters obtained for the SDI interaction are compatible with regularity. We may conclude that the SDI, which provides a simple extension of the schematic shell model [15], does not describe the underlying interactions in the nucleus ^{208}Pb correctly. On the other hand, the M3Y and KB interactions are based on realistic, effective nucleon-nucleon interactions.

However, especially our finding for the levels with unnatural parity differs from those of an analysis of the NNSD based on the same experimental data [1] in terms of the Brody distribution [54], which also depends on a chaoticity parameter [55]. These discrepancies might originate from the fact that the analysis of Ref. [55] did not include long-range correlations. Nevertheless, we obtain chaoticity parameters close to the values for the GOE even when taking into account only the NNSD. To ensure that this discrepancy does not arise from the unfolding procedure, we furthermore evaluated the ratio distributions using ensembles of subspectra comprising the natural and unnatural parity states, respectively. This analysis corroborated the outcome of the calculations with the RMT model Eq. (1) and the method of Bayesian inference.

In conclusion, by analyzing a complete set of levels in ^{208}Pb with unambiguously assigned spin and parity with the RMT model Eq. (1) and the Bayesian method, evidence has been presented for fluctuation properties which are consistent with those of random matrices from the GOE and, thus, for chaoticity of the nuclear system. Similar results were obtained from the analysis of the spectra generated from nuclear model calculations with M3Y and KB interactions. These two models confirm that the chaoticity is caused by a nuclear residual interaction that mixes the configurations inextricably in the many-body system. Indeed, e.g., in the M3Y model, the spectral properties of the unperturbed energy levels, i.e., the diagonal elements of the Hamiltonian H, yielded for the chaoticity parameters $\overline{f} = 0.19$, $\sigma = 0.066$ and $\lambda = 0.09$, $\sigma_\lambda = 0.010$, respectively; that is, they exhibit Poisson statistics—see Fig. 5 of Ref. [45]. These values, actually, are close to those for the SDI interaction. Furthermore, the distance between the unperturbed energy levels for each value of J^π and the perturbed ones, i.e., the eigenvalues of H, is considerably larger than the root-mean square of the off-diagonal interaction matrix elements of H; see Chap. 4 of Ref. [56]. Thus, the SDI interaction seems to be too weak to induce a sufficient mixture of the individual configurations to yield a chaotic dynamics.

We thank T. Guhr, T. T. S. Kuo, and H. A. Weidenmüller for discussions. One of us (A. R.) is grateful to L. Muñoz for providing the article [55] prior to publication. This work was supported by the Deutsche Forschungsgesellschaft (DFG) within the Collaborative Research Centers 634 and 1245. B. A. B. acknowledges U.S. NSF Grant No. PHY-1404442.

*Deceased.
†Dietz@ikp.tu-darmstadt.de
‡A.Heusler@mpi-hd.mpg.de
§Richter@ikp.tu-darmstadt.de
¶brown@nscl.msu.edu

[1] A. Heusler, R. V. Jolos, T. Faestermann, R. Hertenberger, H.-F. Wirth, and P. von Brentano, Phys. Rev. C **93**, 054321 (2016).
[2] M. J. Martin, Nucl. Data Sheets **108**, 1583 (2007).
[3] A. Heusler, T. Faestermann, R. Hertenberger, R. Krücken, H.-F. Wirth, and P. von Brentano, Eur. Phys. J. A **46**, 17 (2010).
[4] A. Heusler, J. Phys. Conf. Ser. **580**, 012021 (2015).
[5] T. T. S. Kuo and G. E. Brown (private communication); https://www.mpi-hd.mpg.de/personalhomes/hsl/Blei208KuoBrown/.
[6] T. T. S. Kuo and G. E. Brown, Nucl. Phys. **85**, 40 (1966).
[7] T. T. S. Kuo, Nucl. Phys. **103**, 71 (1967).
[8] T. T. S. Kuo, J. Blomqvist, and G. E. Brown, Phys. Lett. **31B**, 93 (1970).
[9] W. W. True, C. W. Ma, and W. T. Pinkston, Phys. Rev. C **3**, 2421 (1971).
[10] V. Gillet, A. M. Green, and E. A. Sanderson, Phys. Lett. **11**, 44 (1964).
[11] B. A. Brown, Phys. Rev. Lett. **85**, 5300 (2000).
[12] K. H. Maier, https://www.mpi-hd.mpg.de/personalhomes/hsl/Blei208KHMaier/.
[13] G. Bertsch, J. Borysowicsz, H. McManus, and W. G. Love, Nucl. Phys. **284**, 399 (1977).
[14] G. F. Bertsch and I. Hamamoto, Phys. Rev. C **26**, 1323 (1982).
[15] A. Heusler, R. V. Jolos, and P. von Brentano, Yad. Fiz. **76**, 860 (2013) [Phys. At. Nucl. **76**, 807 (2013)]; https://www.mpi-hd.mpg.de/personalhomes/hsl/Blei208SDI/.
[16] S. A. Moszkowski, Phys. Rev. C **19**, 2344 (1979).
[17] I. Talmi, in *Contemporary Concepts in Physics* (Harwood, Chur, 1993), Vol. 7.
[18] E. K. Warburton and B. A. Brown, Phys. Rev. C **43**, 602 (1991).
[19] A. Bohr and B. R. Mottelson, *Nuclear Structure* (Benjamin, New York, 1969), Vol. I.
[20] M. V. Berry and M. Tabor, Proc. R. Soc. A **356**, 375 (1977).
[21] O. Bohigas, M. J. Giannoni, and C. Schmit, Phys. Rev. Lett. **52**, 1 (1984).
[22] S. W. McDonald and A. N. Kaufman, Phys. Rev. Lett. **42**, 1189 (1979).
[23] G. Casati, F. Valz-Gris, and I. Guarneri, Lett. Nuovo Soc. Ital. Fis. Cimento **28**, 279 (1980).
[24] M. V. Berry, Eur. J. Phys. **2**, 91 (1981).

[25] F. J. Dyson and M. L. Mehta, J. Math. Phys. (N.Y.) **4**, 701 (1963).
[26] M. L. Mehta, *Random Matrices* (Academic Press, London, 1990).
[27] T. Guhr and H. A. Weidenmüller, Ann. Phys. (N.Y.) **193**, 472 (1989).
[28] V. V. Flambaum, A. A. Gribakina, G. F. Gribakin, and M. G. Kozlov, Phys. Rev. A **50**, 267 (1994).
[29] V. Zelevinsky, B. A. Brown, N. Frazier, and M. Horoia, Phys. Rep. **276**, 85 (1996).
[30] J. M. G. Gómez, K. Kar, V. K. B. Kota, R. A. Molina, A. Relaño, and J. Retamosa, Phys. Rep. **499**, 103 (2011).
[31] H. A. Weidenmüller and G. E. Mitchell, Rev. Mod. Phys. **81**, 539 (2009).
[32] G. Lenz and F. Haake, Phys. Rev. Lett. **67**, 1 (1991).
[33] H. Alt, H.-D. Gräf, H. L. Harney, R. Hofferbert, H. Lengeler, C. Rangacharyulu, A. Richter, and P. Schardt, Phys. Rev. E **50**, R1 (1994).
[34] V. K. B. Kota, *Lecture Notes in Physics* (Springer, Heidelberg, 2014), Vol. 884.
[35] A. Y. Abul-Magd and M. H. Simbel, Phys. Rev. C **54**, 1675 (1996).
[36] A. Y. Abul-Magd, H. L. Harney, M. H. Simbel, and H. A. Weidenmüller, Phys. Lett. B **579**, 278 (2004).
[37] A. Y. Abul-Magd, H. L. Harney, M. H. Simbel, and H. A. Weidenmüller, Ann. Phys. (Amsterdam) **321**, 560 (2006).
[38] G. E. Mitchell, E. G. Bilpuch, P. M. Endt, and J. F. Shriner, Jr., Phys. Rev. Lett. **61**, 1473 (1988).
[39] J. F. Shriner, Jr., G. E. Mitchell, and B. A. Brown, Phys. Rev. C **71**, 024313 (2005).
[40] G. E. Mitchell and J. F. Shriner, Jr., Phys. Scr. **T90**, 105 (2001).
[41] S. Raman, T. A. Walkiewicz, S. Kahane, E. T. Jurney, J. Sa, Z. Gácsi, J. L. Weil, K. Allaart, G. Bonsignori, and J. F. Shriner, Jr., Phys. Rev. C **43**, 521 (1991).
[42] J. D. Garrett, J. Q. Robinson, A. J. Foglia, and H.-Q. Jin, Phys. Lett. B **392**, 24 (1997).
[43] O. Bohigas, R. U. Haq, and A. Pandey, in *Nuclear Data for Science and Technology*, edited by K. H. Böckhoff (Reidel, Dordrecht, 1983).
[44] N. Rosenzweig and C. E. Porter, Phys. Rev. **120**, 1698 (1960).
[45] See Supplemental Material at http://link.aps.org/supplemental/10.1103/PhysRevLett.118.012501 for additional figures where the results for the statistical measures obtained from the experimental levels and from those calculated using nuclear models with SDI, M3Y, and KB interactions are compared to the RMT model Eq. (1) evaluated at the values of λ listed in Table I in Figs. 1–3 and to the NNSDs computed with the method of Bayesian inference Eqs. (3) and (5) in Fig. 4. Figure 6 shows the statistical measures obtained for the complete experimental spectrum, that is, when disregarding parity and spin. As expected, they exhibit Poissonian statistics.
[46] A. G. W. Cameron and R. M. Elkin, Can. J. Phys. **43**, 1288 (1965).
[47] A. Gilbert and A. G. W. Cameron, Can. J. Phys. **43**, 1446 (1965).
[48] J. F. Shriner, Jr., G. E. Mitchell, and T. von Egidy, Z. Phys. A **338**, 309 (1991).
[49] Y. Y. Atas, E. Bogomolny, O. Giraud, and G. Roux, Phys. Rev. Lett. **110**, 084101 (2013).
[50] B. Dietz, T. Klaus, M. Miski-Oglu, A. Richter, M. Wunderle, and C. Bouazza, Phys. Rev. Lett. **116**, 023901 (2016).
[51] H. L. Harney, *Bayesian Inference—Parameter Estimation and Decisions* (Springer, Heidelberg, 2003).
[52] H. Jeffrey, Proc. R. Soc. A **186**, 453 (1946).
[53] H. Jeffrey, *Theory of Probability* (Oxford University Press, New York, 1961).
[54] T. A. Brody, J. Flores, J. B. French, P. A. Mello, A. Pandey, and S. S. M. Wong, Rev. Mod. Phys. **53**, 385 (1981).
[55] L. Muñoz *et al.*, Phys. Rev. C (to be published).
[56] T. Guhr, A. Müller-Groeling, and H. A. Weidenmüller, Phys. Rep. **299**, 189 (1998).